Received: 27 June 2023 | Revised: 11 July 2023 | Accepted: 23 August 2023

DOI: 10.1002/pamm.202300054

RESEARCH ARTICLE

Convex reconstruction of moving particles with inexact motion model

Bernadette Hahn[1] | **Benedikt Wirth**[2]

[1]Department of Mathematics, University of Stuttgart, Pfaffenwaldring 57, Stuttgart, Germany

[2]Applied Mathematics, University of Münster, Einsteinstraße 62, Münster, Germany

Correspondence
Benedikt Wirth, Department of Applied Mathematics, University of Münster, Einsteinstraße 62, 48149 Münster, Germany.
Email: Benedikt.Wirth@uni-muenster.de

Funding information
Deutsche Forschungsgemeinschaft

Abstract

We propose a novel convex optimization problem for the reconstruction of temporally moving nonnegative point sources or particles. As in previously developed approaches from the literature, we base our reconstruction on a linear motion model in which particles move at constant d-dimensional velocity. However, in contrast to existing approaches we allow a deviation from the exact linear motion, thereby accounting for the modelling error inherent in that motion model. The deviation is measured with the help of Wasserstein distances and is constrained not to exceed a freely selectable bound which represents the model inexactness. We show well-posedness and first numerical results for the model.

1 | REVIEW OF POINT SOURCE RECONSTRUCTION

The reconstruction of point source configurations from finite precision measurements is a classical inverse or signal analysis problem that can be formulated as follows. The point source configuration is described as an element u of the space $\mathcal{M}_+(\Omega)$ of nonnegative Radon measures on some domain $\Omega \subset \mathbb{R}^d$, more precisely, as a finite linear combination

$$u^\dagger = \sum_{i=1}^{N} m_i \delta_{x_i}$$

of $N \in \mathbb{N}$ Dirac measures at locations $x_1, \dots, x_N \in \Omega$ with positive linear coefficients $m_i \in (0, \infty)$. The measurement is represented by a (typically linear) operator $\mathrm{Ob} : \mathcal{M}(\Omega) \to H$ from the space $\mathcal{M}(\Omega)$ of Radon measures to some Hilbert space H, for instance by a convolution with a smoothing kernel (which is an instance of the more general setting in which H is a reproducing kernel Hilbert space and $\mathrm{Ob}u^\dagger$ yields the Riesz representation of $u^\dagger$, the latter being interpreted as an element of the dual space H^*). Given only the measurement

$$f = \mathrm{Ob}u^\dagger,$$

the task is now to reconstruct $u^\dagger$.

In applications, the point source configuration may for instance represent the mass distribution of fluorescent molecules in fluorescence microscopy or the distribution of radioactively marked leukocytes in a patient [1, 2] or the distribution of ultrasonic reflectors in ultrasonography [3]. The measurement may be indirect as in positron emission tomography (in which case $\mathrm{Ob}u^\dagger$ would be the Radon transform of a smoothed version of $u^\dagger$) or direct as in fluorescence microscopy, but

in any case they typically only have finite precision or resolution: For instance, a microscopy image is always bandlimited due to the diffraction limit. The simplest model for such a finite precision measurement is if the domain Ω is taken to be $[-1,1)^d$ with periodic boundary conditions (the flat torus) and Ob is taken as the *ideal low-pass filter*, which is the Fourier series truncated at some cutoff frequency $\Phi \in \mathbb{N}$,

$$\mathrm{Ob}u = \left(\int_\Omega \exp(-\pi i x \cdot \xi) \, \mathrm{d}u(x) \right)_{\xi \in \mathbb{Z}^d, \|\xi\|_\infty \leq \Phi}.$$

For simplicity, we will in the following restrict to this setting, though everything also extends to other measurement operators of similar type.

It turns out that despite the finite precision measurement one can often reconstruct the original point configuration $u^\dagger$ *exactly* from f, by solving the variational problem

$$\min_{u \in \mathcal{M}_+(\Omega)} \|u\|_{\mathcal{M}} \qquad \text{such that } \mathrm{Ob}u = f,$$

where $\|\cdot\|_{\mathcal{M}}$ denotes the total variation norm on the space of Radon measures. For instance, this is the case if the number N of point sources in $u^\dagger$ is (up to a sufficiently small constant) bounded by Φ^d [4, 5]. Even if one allows complex point masses m_i, one can obtain exact reconstruction, for instance if the locations x_i have mutual distance larger than (a sufficiently big constant times) $\frac{1}{\Phi}$ [6]. If the measurement data f are noisy, the constraint $\mathrm{Ob}u = f$ can be replaced by a penalty, and one may also obtain error estimates for the reconstruction under slightly stronger assumptions on $u^\dagger$. Such error estimates may come in norms dual to reproducing kernel Hilbert space norms [7], in unbalanced optimal transport error measures [8, 9], or in error estimates directly for the locations x_i and masses m_i [4].

2 | REVIEW OF RECONSTRUCTING MOVING POINT SOURCES

In several applications, the point masses to be reconstructed are not static, but move over time, so we have a different point configuration $u_t^\dagger \in \mathcal{M}_+(\Omega)$ at each time $t \in \mathbb{R}$, a so-called *snapshot*. One then has measurements

$$f_t = \mathrm{Ob}u_t^\dagger, \qquad t \in \mathcal{T},$$

at a finite number of time points $\mathcal{T} \subset \mathbb{R}$. In principle, also the measurement operator Ob might depend on time, in particular if the physical measurement comprises several components that are consecutively acquired, as is typical in tomographic imaging, but for notational simplicity we take the same measurement operator at all times. The reason to give this dynamic setting a special treatment (instead of separately reconstructing all snapshots $u_t^\dagger$ on their own) is twofold:

1. One is not only interested in the location and mass of the point sources at the different time points, thus in the reconstruction of the $u_t^\dagger$ for $t \in \mathcal{T}$, but also in some information on the particle velocities (and potentially even in the particle configurations at intermediate times $t \notin \mathcal{T}$).
2. Moreover, it may happen that the snapshot $u_t^\dagger$ cannot be reconstructed from the knowledge of f_t alone, but that actually the information from all other time points is required, combined with some knowledge of the temporal regularity of the particle motion. This is of particular relevance if the observation operator Ob depends on time as well.

Such a reconstruction of dynamically evolving point configurations can be performed based on different (relatively generic) motion models. For example, one can simply penalize (too high) velocities, resulting in optimal transport regularizations for the temporal evolution of $u_t^\dagger$ [2]. A much stronger, but also much more restrictive regularization confines the possible motions to an explicit, small set of possible motions such as linear motions: In [3] (which our method will be based on), each particle is represented by a (weighted) Dirac mass $\delta_{(x_i, v_i)}$ in the 2d-dimensional position velocity space, where $x_i \in \Omega$ and $v_i \in \mathbb{R}^d$ represent the initial particle position and its (constant) velocity, respectively. The temporally evolving particle configuration is thus described by a measure

$$\lambda^\dagger = \sum_{i=1}^N m_i \delta_{(x_i, v_i)} \in \mathcal{M}_+(\Omega \times \mathbb{R}^d),$$

where the particle configuration at time t is given by

$$u_t^\dagger = \sum_{i=1}^N m_i \delta_{x_i + t v_i} \in \mathcal{M}_+(\Omega).$$

The latter can equivalently be expressed as a linear *move operator* $\mathrm{Mv}_t^d : \mathcal{M}(\mathbb{R}^{2d}) \to \mathcal{M}(\mathbb{R}^d)$ applied to $\lambda^\dagger$, which simply forms the pushforward of $\lambda^\dagger$ under the map $(x, v) \mapsto x + tv$,

$$u_t^\dagger = \mathrm{Mv}_t^d \lambda^\dagger = [(x, v) \mapsto x + tv]_\# \lambda^\dagger$$

(the pushforward $\phi_\# \rho$ of a measure ρ under a measurable map ϕ is defined by $\phi_\# \rho(A) = \rho(\phi^{-1}(A))$). In [3], the authors then suggest to solve the following convex variational problem to reconstruct the particle configuration $\lambda^\dagger$,

$$\min_{\substack{\lambda \in \mathcal{M}_+(\Omega \times \mathbb{R}^d) \\ (u_t)_{t \in \mathcal{T}} \subset \mathcal{M}_+(\Omega)}} \|\lambda\|_{\mathcal{M}} \qquad \text{such that } u_t = \mathrm{Mv}^d \lambda \text{ and } \mathrm{Ob} u_t = f_t \text{ for all } t \in \mathcal{T}.$$

They prove that as long as there are no coincidences (which are essentially particle collisions) and no ghost particles (imaginary particles that collide with a different particle at every time $t \in \mathcal{T}$) and the particles have sufficient mutual distance, then this minimization problem reconstructs the true particle configuration $\lambda^\dagger$. In a simplified and discretized setting, they also prove error bounds if the measurements are noisy and thus the measurement constraint is replaced by a penalty.

We will build on a model variant that reduces the dimension of the problem. In more detail, since the sought particle configuration $\lambda^\dagger$ is a measure in a 2d-dimensional and thus very high-dimensional space, a dimension-reduced version of the approach was introduced in [9]: One keeps the unknowns $(u_t)_{t \in \mathcal{T}}$, but instead of the full measure $\lambda \in \mathcal{M}_+(\mathbb{R}^{2d})$ one only considers measures $(\gamma_\theta)_{\theta \in \Theta} \subset \mathcal{M}_+(\mathbb{R}^2)$ for a finite set of directions $\Theta \subset S^{d-1}$. The measure γ_θ shall describe the same linear motions as λ, only projected onto the one-dimensional line spanned by θ, thus

$$\gamma_\theta = [(x, v) \mapsto (x \cdot \theta, v \cdot \theta)]_\# \lambda \qquad \text{or equivalently} \qquad \gamma_\theta = \sum_{i=1}^N m_i \delta_{(x_i \cdot \theta, v_i \cdot \theta)} \text{ if } \lambda = \sum_{i=1}^N m_i \delta_{(x_i, v_i)}.$$

Since both the snapshots u_t as well as the one-dimensional dynamic particle configurations γ_θ derive from the same measure λ, they necessarily satisfy the consistency condition

$$\mathrm{Mv}_t^1 \gamma_\theta = \mathrm{Rd}_\theta u_t \qquad \text{for all } t \in \mathcal{T}, \theta \in \Theta,$$

where Rd_θ denotes the Radon transform in direction θ, thus

$$\mathrm{Rd}_\theta u = [x \mapsto \theta \cdot x]_\# u.$$

The dimension-reduced convex variational problem for reconstructing the snapshots and the one-dimensional dynamic particle configurations then reads

$$\min_{\substack{(u_t)_{t \in \mathcal{T}} \subset \mathcal{M}_+(\Omega) \\ (\gamma_\theta)_{\theta \in \Theta} \subset \mathcal{M}_+(\mathbb{R}^2)}} \sum_{t \in \mathcal{T}} \|u_t\|_{\mathcal{M}} + \sum_{\theta \in \Theta} \|\gamma_\theta\|_{\mathcal{M}} \quad \text{such that } \mathrm{Mv}_t^1 \gamma_\theta = \mathrm{Rd}_\theta u_t \text{ and } \mathrm{Ob} u_t = f_t \text{ for all } t \in \mathcal{T}, \theta \in \Theta. \tag{1}$$

Under essentially the same conditions as for the original model, one obtains exact reconstruction of the true particle configuration and error estimates in case of noisy measurements [9].

3 | A NEW MODEL FOR RECONSTRUCTING MOVING POINT SOURCES WITH INEXACT LINEAR MOTION

In real applications, the previous model assumption of a strictly linear particle motion is too restrictive: Maybe over sufficiently short time intervals, the particle motion could be viewed as approximately linear, but typical particles such as

leukocytes or ultrasonic reflectors in the blood stream deviate too much from this linear motion to apply the model as is. One way out would be to parameterize the allowed motions by more parameters, for instance not only by the initial particle location and velocity, but additionally by an acceleration. However, this would increase the dimension of the sought variables (in particular of the γ_θ), and also it is unclear whether this additional degree of freedom suffices to capture the actually occurring point source motions. An alternative, which we would like to follow here, is to accept the inexactness of the linear motion model and therefore to allow some discrepancy in those constraints that describe the motion: In particular, we suggest to replace the constraint $\mathrm{Mv}_t^1\gamma_\theta = \mathrm{Rd}_\theta u_t$ by the convex inequality constraint

$$W_p(\mathrm{Mv}_t^1\gamma_\theta, \mathrm{Rd}_\theta u_t)^p \le Md(t)^p, \tag{$C_p(t,\theta)$}$$

where $W_p(\mu,\nu)$ denotes the Wasserstein-p distance between two nonnegative measures μ and ν for $p \ge 1$, $M > 0$ is an estimate of the total particle mass $\sum_{i=1}^N m_i$ (which may also be replaced by $u_t(\Omega)$ or $\gamma_\theta(\mathbb{R}^2)$ without compromising convexity) and $d(t)$ describes the distance by which a particle is allowed to deviate at time t from the linear motion path. The Wasserstein-p distance is a metric on the space of nonnegative Radon measures of fixed mass on some domain D, defined by

$$W_p(\mu,\nu)^p = \inf_{\pi\in\mathcal{M}_+(D\times D)} \int_{D\times D} |x-y|^p \,\mathrm{d}\pi(x,y) \qquad \text{such that } \mathrm{pr}_{1\#}\pi = \mu,\ \mathrm{pr}_{2\#}\pi = \nu,$$

where $\mathrm{pr}_1(x,y) = x$ and $\mathrm{pr}_2(x,y) = y$ denote the projection onto the first and second variable, respectively. It measures the cost for transporting the mass of μ onto ν, where $\pi(A,B)$ has the interpretation of how much mass of μ will be transported from A to B and the constraints ensure that indeed μ is transported onto ν. If $\mu = \sum_{i=1}^N m_i\delta_{x_i}$ and $\nu \sum_{i=1}^N m_i\delta_{\tilde{x}_i}$ represent discrete measures with $\tilde{x}_i$ sufficiently close to x_i, then it evaluates to

$$W_p\left(\sum_{i=1}^N m_i\delta_{x_i}, \sum_{i=1}^N m_i\delta_{\tilde{x}_i}\right)^p = \sum_{i=1}^N m_i|x_i-\tilde{x}_i|^p,$$

for which the so-called *coupling measure* is given by $\pi = \sum_{i=1}^N m_i\delta_{(x_i,\tilde{x}_i)}$. The new constraint ensures that, at least on average, a particle visible in u_t never deviates from the linear motion encoded in γ_θ by more than distance $d(t)$. Note that taking the formal limit $p \to \infty$ one can define

$$W_\infty(\mu,\nu) = \min_{\pi\in\mathcal{M}_+(D\times D)} \sup_{(x,y\in\mathrm{supp}\,\pi)} |x-y| \qquad \text{such that } \mathrm{pr}_{1\#}\pi = \mu,\ \mathrm{pr}_{2\#}\pi = \nu,$$

and therefore would formulate the inequality constraint in this case rather as

$$W_\infty(\mathrm{Mv}_t^1\gamma_\theta, \mathrm{Rd}_\theta u_t) \le d(t). \tag{$C_\infty(t,\theta)$}$$

Summarizing, we propose to reconstruct the dynamic particle configuration by solving the convex variational program

$$\min_{\substack{(u_t)_{t\in\mathcal{T}}\subset\mathcal{M}_+(\Omega)\\(\gamma_\theta)_{\theta\in\Theta}\subset\mathcal{M}_+(\mathbb{R}^2)}} \sum_{t\in\mathcal{T}} \|u_t\|_{\mathcal{M}} + \sum_{\theta\in\Theta} \|\gamma_\theta\|_{\mathcal{M}} \text{ such that } (C_p(t,\theta)) \text{ and } \mathrm{Ob}u_t = f_t \text{ hold for all } t\in\mathcal{T}, \theta\in\Theta \tag{2}$$

with $1 \le p \le \infty$. The well-posedness of this minimization problem is straightforward if the constraints can be satisfied, that is, if the measurements f_t really come from masses that move approximately linearly with a deviation of at most $d(t)$.

Theorem 3.1 (Existence of minimizers). *If there exist $(u_t^n)_{t\in\mathcal{T}}$, $(\gamma_\theta^n)_{\theta\in\Theta}$ such that the constraints can be satisfied, problem (2) has a solution.*

Proof. Consider a minimizing sequence $(u_t^n)_{t\in\mathcal{T}}$, $(\gamma_\theta^n)_{\theta\in\Theta}$ for $n = 1, 2, \ldots$. Due to the boundedness of the energy along this sequence, we have boundedness of $\|u_t^n\|_{\mathcal{M}}$ and $\|\gamma_\theta^n\|_{\mathcal{M}}$ for all $t\in\mathcal{T}$ and $\theta\in\Theta$. By Banach–Alaoglu, there exists a subsequence, still indexed by n, such that $u_t^n \overset{*}{\rightharpoonup} u_t$ and $\gamma_\theta^n \overset{*}{\rightharpoonup} \gamma_\theta$ weakly-$*$ as $n\to\infty$ for all $t\in\mathcal{T}$ and $\theta\in\Theta$ and some $(u_t)_{t\in\mathcal{T}} \subset \mathcal{M}_+(\Omega)$, $(\gamma_\theta)_{\theta\in\Theta} \subset \mathcal{M}_+(\mathbb{R}^2)$. Since the ideal low-pass filter Ob is continuous with respect to weak-$*$ convergence, the measurement constraints stay satisfied in the limit. Similarly, $\mathrm{Mv}_t^1\gamma_\theta^n \overset{*}{\rightharpoonup} \mathrm{Mv}_t^1\gamma_\theta$ and $\mathrm{Rd}_\theta u_t^n \overset{*}{\rightharpoonup} \mathrm{Rd}_\theta u_t$ due to

the linearity and boundedness of Mv_t^1 and Rd_θ. Furthermore, the Wasserstein-p distance is lower semicontinuous under weak-$*$ convergence (for $p < \infty$ it is even known to metrize weak-$*$ convergence) so that the constraint $(C_p(t,\theta))$ also stays satisfied in the limit, thus $(u_t)_{t\in\mathcal{T}} \subset \mathcal{M}_+(\Omega)$, $(\gamma_\theta)_{\theta\in\Theta} \subset \mathcal{M}_+(\mathbb{R}^2)$ is admissible. Finally, the total variation norm $\|\cdot\|_{\mathcal{M}}$ is weakly-$*$ lower semicontinuous so that $(u_t)_{t\in\mathcal{T}} \subset \mathcal{M}_+(\Omega)$, $(\gamma_\theta)_{\theta\in\Theta} \subset \mathcal{M}_+(\mathbb{R}^2)$ has lower energy than the minimizing sequence and thus is a minimizer. □

Due to convexity, any local minimizer is also a global one, though it might not be unique due to the lack of strict convexity.

4 | OPTIMAL TRANSPORT CONSTRAINTS FOR $p \in \{1, \infty\}$

Inserting the definition of W_p in $(C_p(t,\theta))$ obviously adds the coupling measures $(\pi_{t,\theta})_{t\in\mathcal{T},\theta\in\Theta} \subset \mathcal{M}_+(\mathbb{R}^2)$ as a further auxiliary variable in (2) and the equality constraints of W_p as further auxiliary constraints, resulting in the overall linear program

$$\min_{\substack{(u_t)_{t\in\mathcal{T}}\subset\mathcal{M}_+(\Omega)\\(\gamma_\theta)_{\theta\in\Theta}\subset\mathcal{M}_+(\mathbb{R}^2)\\(\pi_{t,\theta})_{t\in\mathcal{T},\theta\in\Theta}\subset\mathcal{M}_+(\mathbb{R}^2)}} \sum_{t\in\mathcal{T}} \|u_t\|_{\mathcal{M}} + \sum_{\theta\in\Theta} \|\gamma_\theta\|_{\mathcal{M}} \quad \text{such that for all } t\in\mathcal{T}, \theta\in\Theta \text{ it holds}$$

$$\int_{\mathbb{R}^2} \left(\frac{|x-y|}{d(t)}\right)^p \mathrm{d}\pi_{t,\theta}(x,y) \le M,\ \mathrm{pr}_{1\#}\pi_{t,\theta} = \mathrm{Mv}_t^1\gamma_\theta,\ \mathrm{pr}_{2\#}\pi_{t,\theta} = \mathrm{Rd}_\theta u_t,\ \mathrm{Ob}u_t = f_t,$$

where for $p = \infty$, we shall use the notational convention that $r^p = \infty$ for $r > 1$, $1^\infty = 1$, and $r^p = 0$ for $0 \le r < 1$.

Note that the feasibility of the optimal transport subproblems strongly depends on the dimension-reduced setting, since we only need to compare the one-dimensional measures $\mathrm{Mv}_t^1\gamma_\theta$ and $\mathrm{Rd}_\theta u_t$ via optimal transport. In the full-dimensional version from [3], we would have optimal transport subproblems between the d-dimensional measures $\mathrm{Mv}_t^d\lambda$ and u_t, which are known to be computationally highly demanding (one would have to use dynamic or entropically regularized optimal transport versions to approximate such optimal transport problems). In particular, our new additional constraints $\mathrm{pr}_{1\#}\pi_{t,\theta} = \mathrm{Mv}_t^1\gamma_\theta$ and $\mathrm{pr}_{2\#}\pi_{t,\theta} = \mathrm{Rd}_\theta u_t$ have the same complexity as the constraint $\mathrm{Mv}_t^1\gamma_\theta = \mathrm{Rd}_\theta u_t$ in the original model (1) with exact linear motion: In both settings, those are just equalities in $\mathcal{M}_+(\mathbb{R})$.

In the special case of $p \in \{1, \infty\}$, the new model is particularly efficient to implement, since one can strongly reduce the complexity of the auxiliary variable $(\pi_{t,\theta})_{t\in\mathcal{T},\theta\in\Theta}$. Indeed, for $p = \infty$, the integrand $(\frac{|x-y|}{d(t)})^p$ is infinite outside

$$D(t) = \{(x,y) \in \mathbb{R}^2 \mid |x-y| \le d(t)\}$$

so that one may consider $\pi_{t,\theta} \in \mathcal{M}_+(D(t))$ instead of $\pi_{t,\theta} \in \mathcal{M}_+(\mathbb{R}^2)$. If $d(t)$ is of the order of few pixels or voxels (after discretization), then the collection of these $\pi_{t,\theta}$ is actually smaller in size than the collection of the variables u_t and γ_θ.

For $p = 1$ there exists an alternative, so-called *Beckmann formulation* of the Wasserstein distance,

$$W_1(\mu,\nu) = \min_{v\in\mathcal{M}(\mathbb{R}^d)^d} \|v\|_{\mathcal{M}} \qquad \text{such that } \mathrm{div}v = \mu - \nu \text{ (in the distributional sense).}$$

Inserting this in $(C_p(t,\theta))$ turns the model (2) into the linear program

$$\min_{\substack{(u_t)_{t\in\mathcal{T}}\subset\mathcal{M}_+(\Omega)\\(\gamma_\theta)_{\theta\in\Theta}\subset\mathcal{M}_+(\mathbb{R}^2)\\(v_{t,\theta})_{t\in\mathcal{T},\theta\in\Theta},(V_{t,\theta})_{t\in\mathcal{T},\theta\in\Theta}\subset\mathcal{M}(\mathbb{R})}} \sum_{t\in\mathcal{T}} \|u_t\|_{\mathcal{M}} + \sum_{\theta\in\Theta} \|\gamma_\theta\|_{\mathcal{M}} \quad \text{such that for all } t\in\mathcal{T}, \theta\in\Theta \text{ it holds}$$

$$\mathrm{div}v_{t,\theta} = \mathrm{Mv}_t^1\gamma_\theta - \mathrm{Rd}_\theta u_t,\ v_{t,\theta} \le V_{t,\theta},\ -v_{t,\theta} \le V_{t,\theta},\ V_{t,\theta}(\mathbb{R}^2) \le Md(t),\ \mathrm{Ob}u_t = f_t.$$

Again, the auxiliary variables $(v_{t,\theta})_{t\in\mathcal{T},\theta\in\Theta}$ and $(V_{t,\theta})_{t\in\mathcal{T},\theta\in\Theta}$ are smaller in size than the collection of $(u_t)_{t\in\mathcal{T}}$ and $(\gamma_\theta)_{\theta\in\Theta}$.

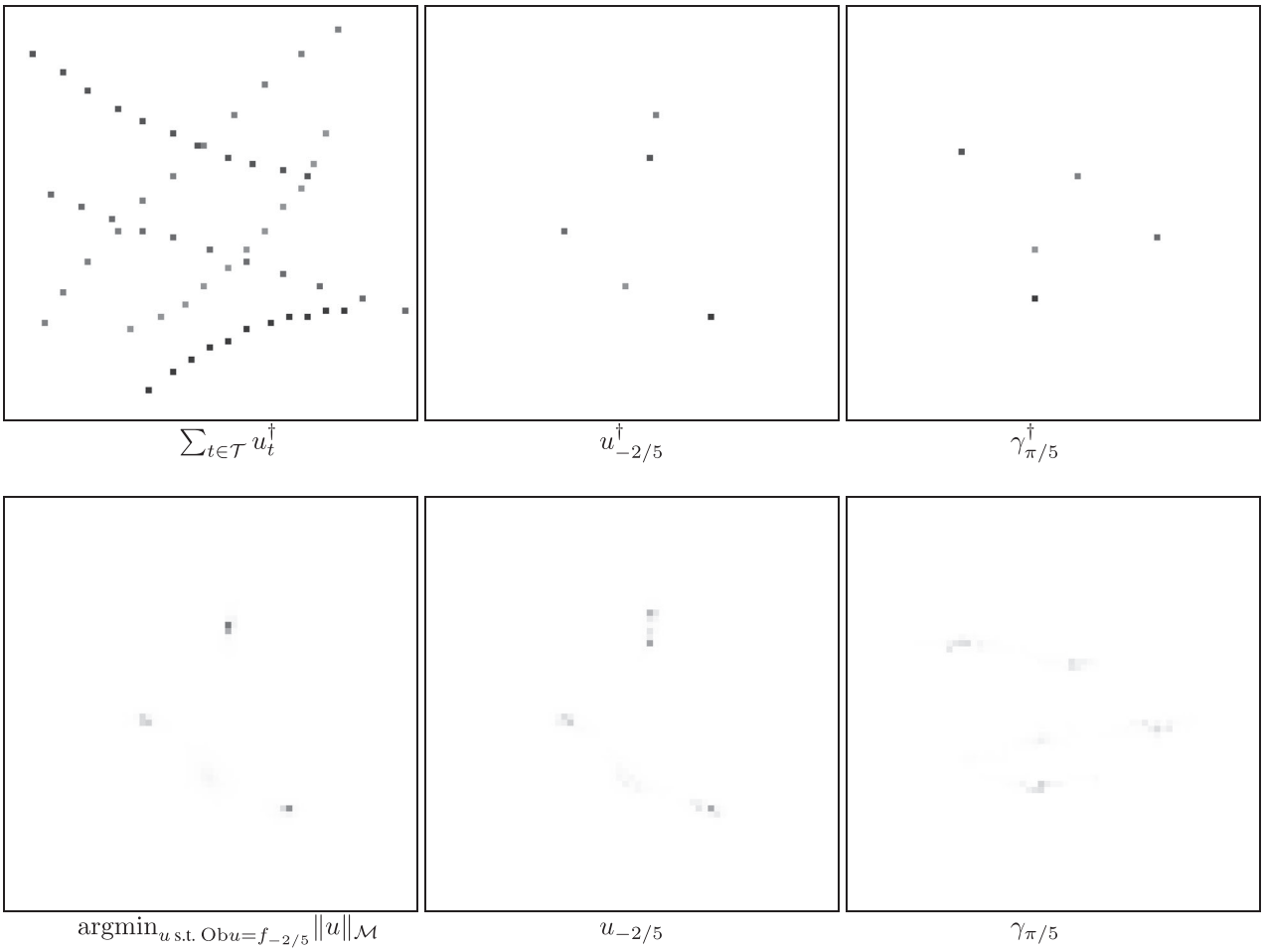

FIGURE 1 Reconstruction results for five moving particles. Top: Ground truth configuration, showing the particle paths (left), a snapshot (middle), and projection of the dynamic particle configuration onto a one-dimensional position-average velocity space (right). Bottom: Reconstruction of the snapshot based solely on the measurement at a single time point (left), reconstruction of the snapshot by our method (middle), and reconstruction of the one-dimensional position-velocity space by our method (right). In both $u_{-2/5}$ and $\gamma_{\pi/5}$, all particles can be seen near their correct locations (the gray values are strongly reduced due to the blur in the solution, which is induced by discretization artifacts and the nonuniqueness of the solution); note that the smallest particle is hardly visible. The single time point reconstruction in the bottom left however cannot separate the particles properly.

5 | NUMERICAL PROOF OF CONCEPT IN TWO SPACE DIMENSIONS

For a numerical proof of concept in two space dimensions, we consider the weakest constraint of the family $(C_p(t,\theta))$ for $p \in [1,\infty]$; that is, we set $p = 1$. Higher values of p (in particular the efficient alternative $p = \infty$) constrain the admissible set further and may thereby single out better solutions (any solution for $p > 1$ is also a solution for $p = 1$). As cutoff frequency, we choose $\Phi = 2$, and we pick $\mathcal{T}$ as 11 equispaced time points between -1 and 1 as well as $\Theta = \{0, \frac{\pi}{5}, \dots, \frac{4\pi}{5}\}$. (Note that the total mass f_0 of all particles belongs to the measurement so that, in this particular simulation, the value of the cost functional in (2) is already fixed by the measurement.) We discretize the u_t via a regular rectangular 65×65 grid on $[-1,1]^2$ and the γ_θ via a regular rectangular 65×65 grid on $[-\sqrt{2},\sqrt{2}]^2$. Consequently, the $v_{t,\theta}$ and $V_{t,\theta}$ are discretized by a regular grid of 65 nodes on $[-\sqrt{2},\sqrt{2}]$. For the allowed deviation from linear motion we choose $d(t) = 0.2t^2$. The code is available at https://github.com/CRC-DIP/inexact-linear-tracking.

Figure 1 shows the reconstruction result for a configuration of five nonlinearly moving particles. We compare our method to the reconstruction of snapshots based solely on the measurement at a single time point. For most time points, this single time point reconstruction yields results almost as good as provided by our method, but there are a few times, such as the one displayed, where it does not manage to properly separate all particles. Our method however reconstructs all particles near their correct locations. From the reconstructed γ_θ, one can see that also the particle velocities are appro-

priately estimated. Nevertheless, the reconstruction exhibits substantial blur which probably is due to two effects: The discretization does not allow to position the particles in their exact ground truth positions, and also due to our inexact motion model there is a little bit of ambiguity in the particle positioning. As a consequence, the smallest particle is only faintly visible in our visualization of the reconstruction.

Obvious questions to be addressed in future work include the following:

- Can one consider some notion of exact reconstruction even in this setting with inexact motion model?
- Does exact reconstruction hold in a certain sense?
- Can one prove stability of the reconstruction with respect to measurement noise, despite the potential nonuniqueness?
- Can one adapt the model for reconstruction under measurement noise and prove corresponding convergence rates?
- What discretizations or model variations can lead to reduced blur in the reconstructions?

ACKNOWLEDGMENTS

This work was supported by the Deutsche Forschungsgemeinschaft (DFG, German Research Foundation) via project 431460824—Collaborative Research Center 1450 and via Germany's Excellence Strategy project 390685587—Mathematics Münster: Dynamics-Geometry-Structure.

Open access funding enabled and organized by Projekt DEAL.

ORCID

Benedikt Wirth https://orcid.org/0000-0003-0393-1938

REFERENCES

1. Lee, K. S., Kim, T. J., & Pratx, G. (2015). Single-cell tracking with PET using a novel trajectory reconstruction algorithm. *IEEE Transactions on Medical Imaging*, *34*(4), 994–1003.
2. Schmitzer, B., Schäfers, K., & Wirth, B. (2020). Dynamic cell imaging in pet with optimal transport regularization. *IEEE Transactions on Medical Imaging*, *39*(5), 1626–1635.
3. Alberti, G. S., Ammari, H., Romero, F., & Wintz, T. (2019). Dynamic spike superresolution and applications to ultrafast ultrasound imaging. *SIAM Journal on Imaging Sciences*, *12*(3), 1501–1527.
4. Denoyelle, Q., Duval, V., & Peyré, G. (2017). Support recovery for sparse super-resolution of positive measures. *The Journal of Fourier Analysis and Applications*, *23*(5), 1153–1194.
5. de Castro, Y., & Gamboa, F. (2012). Exact reconstruction using Beurling minimal extrapolation. *Journal of Mathematical Analysis and Applications*, *395*(1), 336–354.
6. Candès, E. J., & Fernandez-Granda, C. (2014). Towards a mathematical theory of super-resolution. *Communications on Pure and Applied Mathematics*, *67*(6), 906–956.
7. Candès, E. J., & Fernandez-Granda, C. (2013). Super-resolution from noisy data. *The Journal of Fourier Analysis and Applications*, *19*(6), 1229–1254.
8. Wirth, B., & Holler, M. (2023). Exact reconstruction and reconstruction from noisy data: Going beyond point sources? In S. Arridge, M. Burger, B. Hahn, & E. T. Quinto (Eds.), *Tomographic inverse problems: Mathematical challenges and novel applications*. Oberwolfach Workshop Reports (Vol. 2318) Mathematisches Forschungsinstitut Oberwolfach.
9. Holler, M., Schlüter, A., & Wirth, B. (2021, December). Dimension reduction, exact recovery, and error estimates for sparse reconstruction in phase space. *arXiv e-prints*, arXiv:2112.09743.

How to cite this article: Hahn, B., & Wirth, B. (2023). Convex reconstruction of moving particles with inexact motion model. *Proceedings in Applied Mathematics and Mechanics*, *23,* e202300054. https://doi.org/10.1002/pamm.202300054